Support Information

A Novel Flame-Resistant Separator for High Performance Lithium-Sulfur Battery

Jianyi Wang†[a], Menghui Chen†[c], Weiwei Qin *[a,b], Meng Zhou[b]

[a] *Faculty of Geosciences and Environmental Engineering, Southwest Jiaotong University, Chengdu 611756, China*

[b] *Chemical and Materials Engineering Department, New Mexico State University, Las Cruces, NM 88003, USA*

[c] *Institute for Sustainable Energy/College of Sciences, Shanghai University, Shanghai, 200444, China*

† These authors contributed equally.

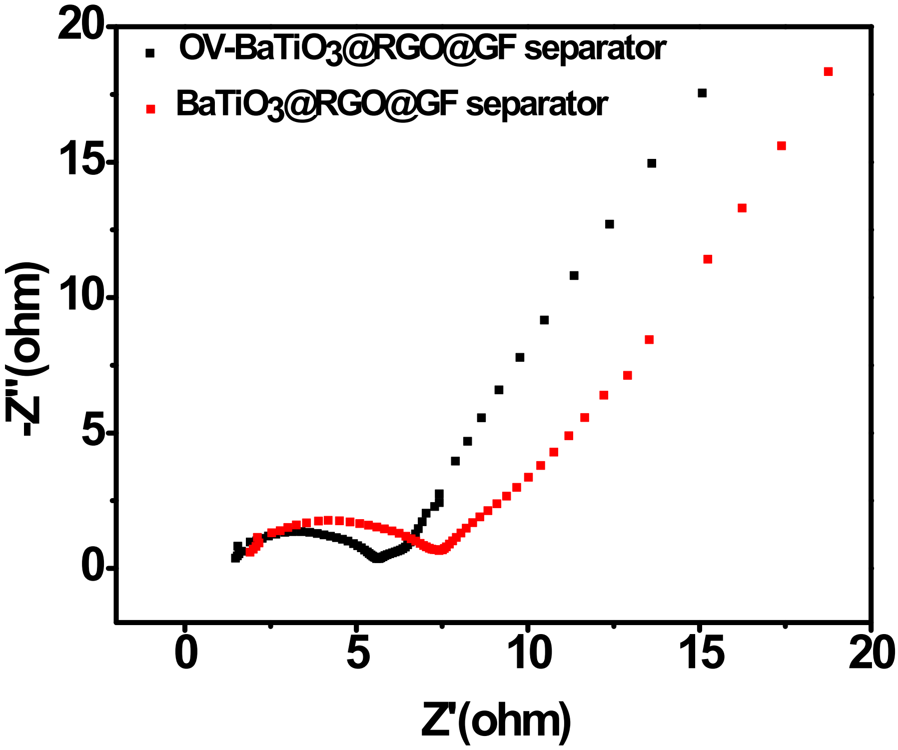

Figure S1 Electrochemical Impedance Spectroscopy (EIS) after 200 cycles of the different $BaTiO_3$–based separators in LSB and inset is corresponding the equivalent-circuit diagram.

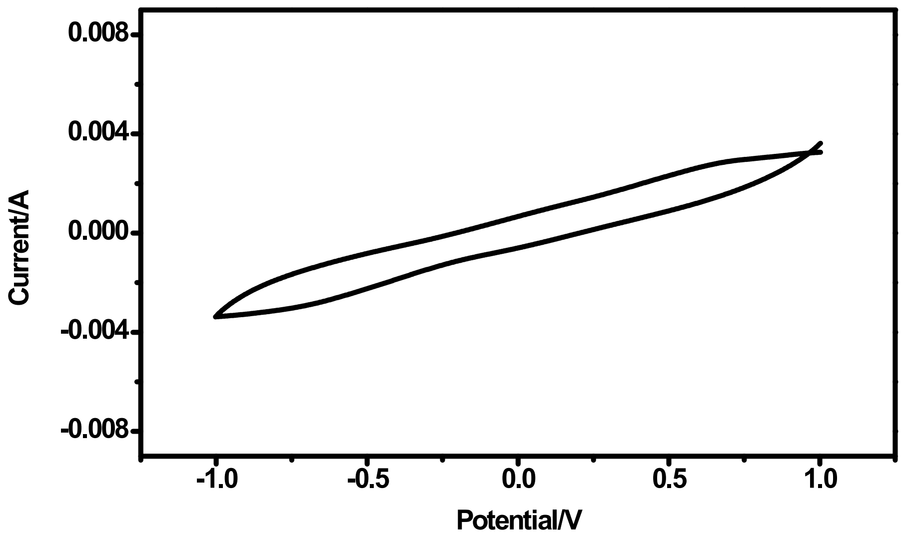

Figure S2 CV curves of the symmetric cells with cathode of RGO in an electrolyte with Li_2S_6 at 10 mV s^{-1}.

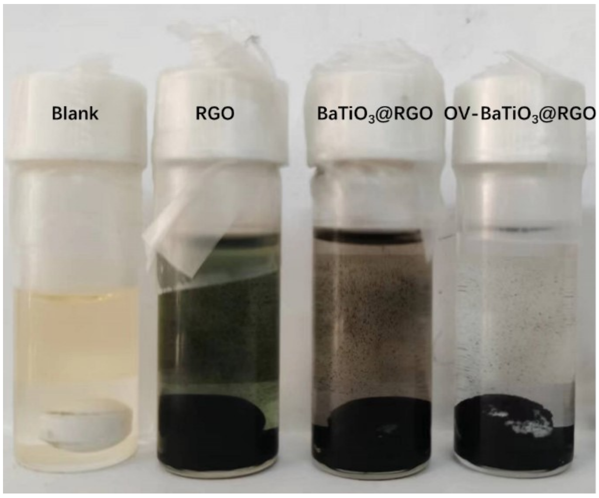

Figure S3 The photograph of sealed vials containing of polysulfides solution after adsorption for one day with different materials of separator coating.

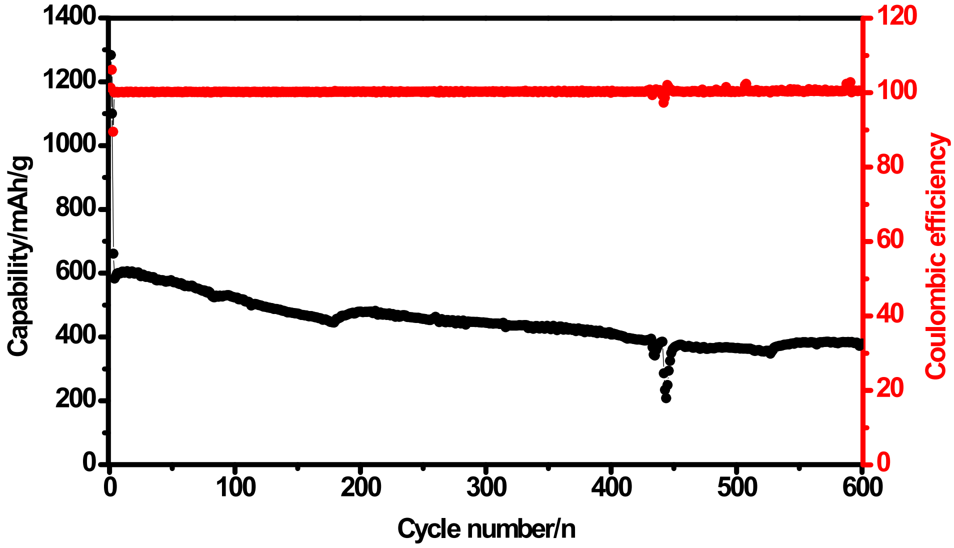

Figure S4 Cycling performance of OV-$BaTiO_3$@RGO@GF separator at a 2 A g^{-1} rate for 600 cycles.

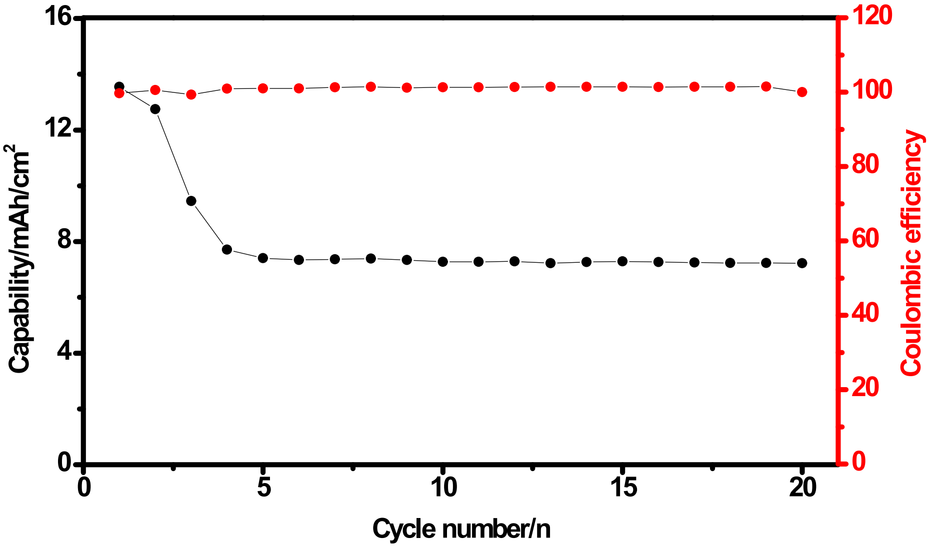

Figure S5 Cycling performance of OV-$BaTiO_3$@RGO@GF separator at a 0.2 A g^{-1} rate under a high loading of 10 mg cm^{-2}.

Figure S6 The OV-$BaTiO_3$@RGO@PP separator c after heat treatment.

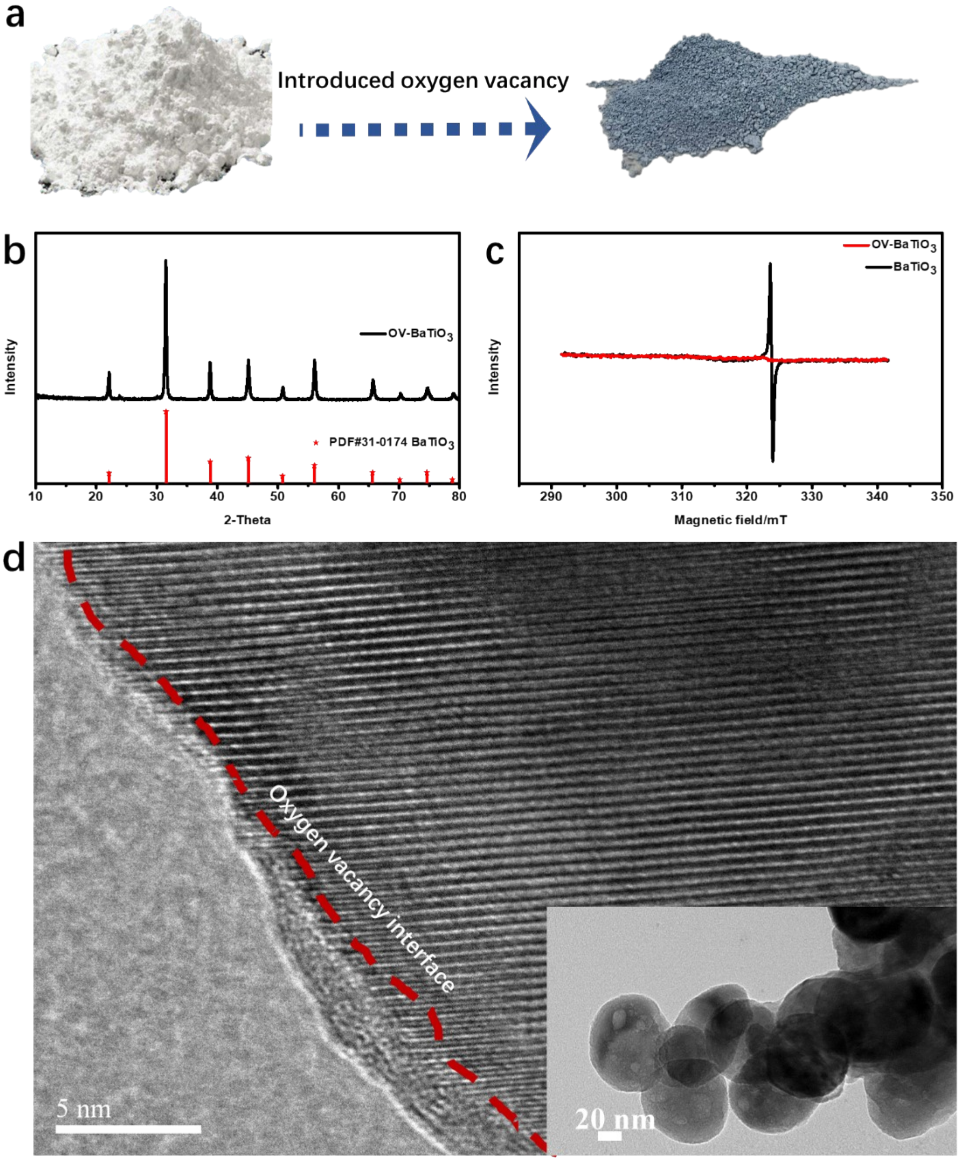

Figure S7 (a) Photograph of pristine and oxygen vacancy of $BaTiO_3$ (OV-$BaTiO_3$). (b) XRD patterns of OV-$BaTiO_3$. (c)EPR of $BaTiO_3$ and OV-$BaTiO_3$. (d) HR-TEM image of OV-$BaTiO_3$ and TEM image of OV-$BaTiO_3$ at bottom left, respectively.

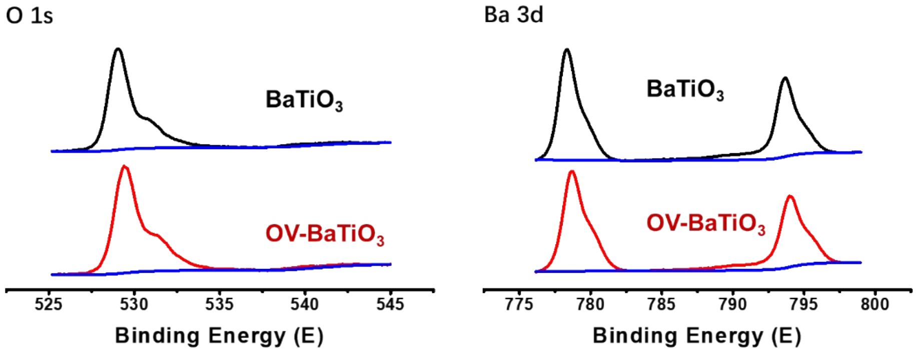

Figure S8 Comparing pristine $BaTiO_3$ and OV-$BaTiO_3$: O1s and Ba_3d XPS spectra.